Talanta 222 (2021) 121484

Contents lists available at ScienceDirect

Talanta

journal homepage: www.elsevier.com/locate/talanta

Stretchable gold fiber-based wearable textile electrochemical biosensor for lactate monitoring in sweat

Ren Wang [a,b], Qingfeng Zhai [a,b], Tiance An [a,b], Shu Gong [a,b], Wenlong Cheng [a,b,*]

[a] Department of Chemical Engineering, Faculty of Engineering, Monash University, Clayton, 3800, Victoria, Australia
[b] The Melbourne Centre for Nanofabrication, 151 Wellington Road, Clayton, 3168, Victoria, Australia

ARTICLE INFO

Keywords:
Lactate biosensor
Smart textile
Gold fiber
Wearable electrochemical sensor
Stretchable electrodes

ABSTRACT

Past several years have witnessed growing interest in developing wearable biosensors for non-invasive monitoring vital signs of chemical/biological markers such as lactate. In this context, textiles can be seen as a promising platform for the integration of wearable chemical sensors due to their inherent breathability, flexibility, softness and comfortableness. Gold is regarded as a preferred active sensing material due to its excellent biocompatibility, chemical inertness and wide electrochemical window. Here, a dry-spinning method was used to fabricate stretchable, strain-insensitive and highly conductive gold fibers. Such gold fibers could be used to fabricate lactate-sensing working electrodes, reference electrode, counter electrodes and further weaved into textiles in a standard three-electrode system with a planar layout. The textile lactate biosensors showed a high sensitivity of 19.13 μA/mM cm^2 in phosphate-buffered solution (PBS) and 14.6 μA/mM cm^2 in artificial sweat. This sensitivity could be maintained under high tensile strain up to 100% without external structural design. The results presented here indicate the potential application of wearable smart textile towards non-invasive lactate monitoring.

1. Introduction

Wearable chemical biosensors have recently received tremendous attention for next-generation non-invasive health monitoring, as they can potentially provide biometric information of chemical and biological species from human bio-fluid in the out-of-hospital environments [1–8]. The level of lactate acids in the bio-fluid is an important health indicator because they are related to several diseases, such as heart failure, circulatory failure, hypoxia, metabolic disorders, respiratory and renal failure [9]. In addition, lactate level is also a crucial indicator for sport tracking because it correlates with the decay of activities. Blood and sweat lactate level in healthy people at rest condition are about 0.5–1.5 mM and 5–25 mM, respectively [10]. Therefore, it can offer enormous benefits if lactate level can be monitored in real-time and in a non-invasive manner.

Past several years have witnessed encouraging progress in developing wearable lactate biosensors. Since the first wearable electrochemical lactate sensor reported [11], there are increasing numbers of researchers attempting to develop wearable electrochemical lactate sensing device [12–16], as electrochemical technology provide easy operation, continuous signal and fast response time [17,18]. It could enable non-invasive, in-situ and real-time monitoring biomarkers from sweat without disrupting skin normal physiological activity. Among them, lactate oxidase (LOx) enzyme-based three-electrode electrochemical system has been developed to monitor lactate level from perspiration, which can be patch based design or fiber/textile based design. The patch-based wearable sensors were most popular configuration, showing easy assembling and operation properties. An integrated multi-sensing system was fabricated by coating bio-receptors on PET patch and it can be mounted onto human skin for in situ lactate analysis. By mounting the patch onto skin, the concentration of different metabolites from sweat could be recorded and transferred to personal smart phone during exercises [16]. As for the textile-based design, the advantage lies at its facile integration with everyday clothing without disturbing daily activities [19–21]. For example, by the knitting and weaving technologies, textile-based wearable electrochemical devices have been integrated onto T-shirt for non-invasive monitoring glucose and lactate in sweat [22]. Another state-of-the-arts example uses multiplex patch-based chemical sensors assembled into a textile, which exhibited good on-body lactate sensing performance by the hierarchical woven and porous structures. The concentration in a volunteer's perspiration was monitored by this sweat patch during excise and the

* Corresponding author. Department of Chemical Engineering, Faculty of Engineering, Monash University, Clayton, 3800, Victoria, Australia.
E-mail address: wenlong.cheng@monash.edu (W. Cheng).

https://doi.org/10.1016/j.talanta.2020.121484
Received 10 March 2020; Received in revised form 11 July 2020; Accepted 29 July 2020
Available online 11 August 2020

results were comparable with commercial high-performance liquid chromatography–mass spectrometry (HPLC-MS) [15]. Nevertheless, one key requirement is that lactate sensing performance needs to be maintained under various deformations of normal skin movement including bending, twisting, or even stretching.

Thus, it is in great need to develop stretchable fiber or textile based wearable electrochemical devices to monitor lactate from sweat, as it can be easily integrated into fabrics for next-generation wearable applications, holding 'unfeelable' experience [23,24]. However, it is nontrivial to fabricate a highly stretchable lactate enzyme biosensors due to the rigid electrode's materials adopted [25]. Although good detection performances of lactate sensing devices have been shown, the stretchability of those lactate sensors are insufficient to accommodate skin deformation [11,13,26]. Consequently, it still remains a great challenge to build a stretchable lactate textile electrochemical biosensor using stretchable and biocompatible material to monitor health related information.

Recently, our group has successfully designed stretchable gold nanomaterial electrodes in the form of nanopatches [27,28], fibers [29] and electronic tattoos [30]. In comparison to other active materials, gold offers the advantages of high chemical inertness, easy surface modification, great biocompatibility and wide electrochemical window [31,32]. Driven by these attributes, we have successfully demonstrated several stretchable electrochemical biosensors including patch-based glucose and cationic ion sensors [33,34], tattoo-based multi-sensor [30] and fiber-based glucose and pH sensors [35,36].

Here, we further explore the potential of our stretchable gold fiber electrodes by designing a stretchable enzymatic textile for real-time lactate monitoring (Fig. 1a). A wearable electrochemical lactate textile is assembled by weaving three different functioned stretchable gold fiber electrodes into a textile to monitor lactate concentration in PBS and artificial sweat, which is the stretchable fiber-based textile lactate biosensor that could be integrated with everyday clothing for comfortable wearing. As illustrated in Fig. 1b–d, a Prussian blue (PB)/LOx/chitosan (CS) coated gold fiber, an elastomeric gold fiber and an Ag/AgCl coated gold fiber served as working, counter and reference electrode, respectively. This enzyme-based electrochemical biosensing system is highly specific yet with an excellent sensitivity of 19.13 μA/mM cm^2 and a low limit of detection (LOD) at 0.137 mM in PBS and 14.6 μA/mM cm^2 in artificial sweat. More importantly, it can maintain its high performance under a large strain up to 100% in both solutions, which is the highest stretchable wearable lactate electrochemical biosensor to the best of our knowledge (Table S2). As a proof of concept, the lactate textile can be used to monitor fitness level from a volunteer's sweat and also can be assembled into glove for soft robotic applications. Our results indicate the potential of gold fiber-based textile as wearable electronics for real-time lactate monitoring in the future.

2. Experiment section

Chemicals and Materials. Gold chloride trihydrate ($HAuCl_4 \cdot 3H_2O$), sodium borohydride ($NaBH_4$), oleylanmine (OA), triisopropylsilane (TIPS), silicon oil, L-ascorbic acid (L-AA), 4-mercaptobenzoic acid (MBA), potassium ferrocyanide (III) ($K_3Fe(CN)_6$), potassium hexacyannoferrate ($K_4Fe(CN)_6$), KCl, NaCl, KNO_3, $FeCl_3$, NH_4Cl, $CaCl_2$, $MgCl_2$, Na_2HPO_4, NaH_2PO_4, $AgNO_3$, glucose, sodium L-Lactate, LOx from *Aerococcus viridans*, urea, uric acid, CS, polyvinyl butyral (PVB) were purchased from Sigma-Aldrich. Styrene-ethylene/butylene-syrene

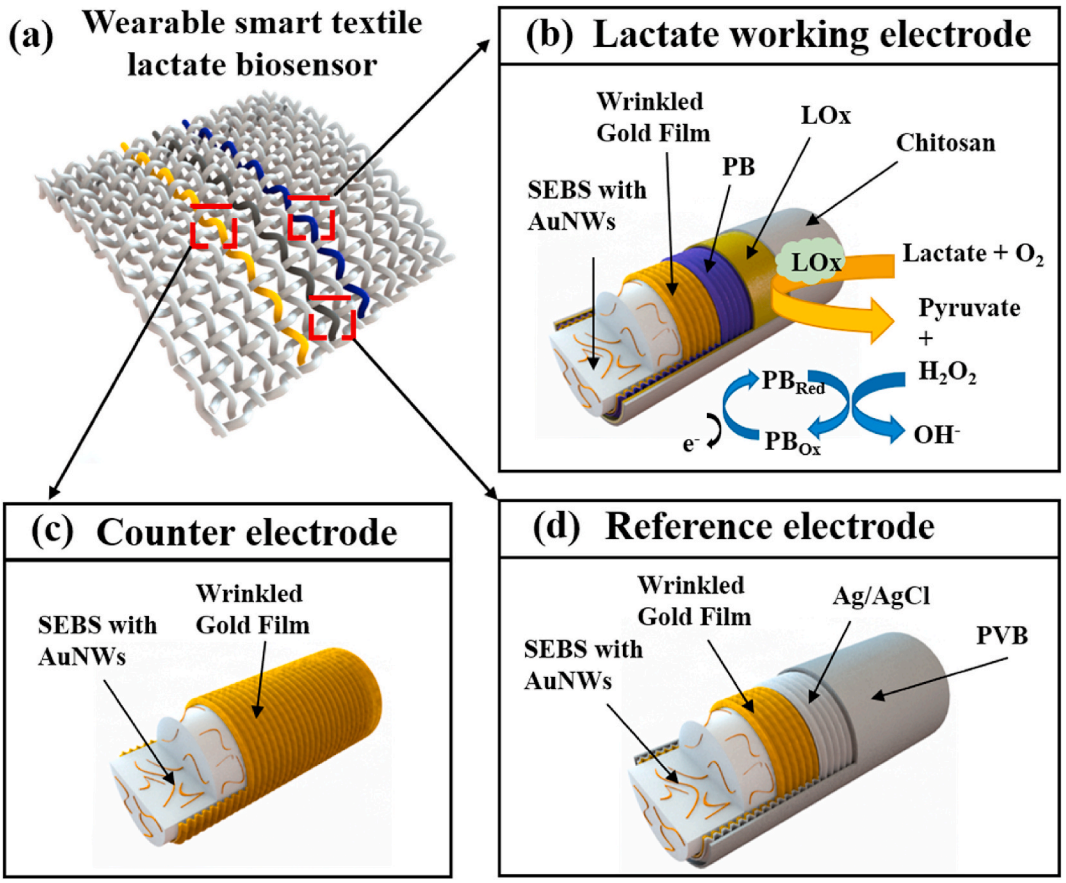

Fig. 1. (a) Scheme of the wearable smart textile electrochemical biosensor toward lactate monitoring. (b) The morphology and mechanism of lactate working electrode. (c) The morphology of elastomeric gold fiber and it can act as a counter electrode directly. (d) The morphology of PVB coated Au/Ag/AgCl reference electrode. (For interpretation of the references to color in this figure legend, the reader is referred to the Web version of this article.)

(SEBS) (G1651H) was purchased from Kraton. N-hexane, acetic acid and methanol were purchased from Merck. Tetra-hydrofuran (THF) and ethanol were purchased from Thermo Fisher Scientific. Sulfuric acid (H_2SO_4) and hydrochloric acid (HCl) were purchased from J.T Baker. Pure orange juice was bought from local supermarket. Au electroless growth solution contained 12 mM $HAuCl_4{\cdot}3H_2O$, 1.1 mM MBA, and 29.1 mM L-AA in water/ethanol solution. Standard 0.1 M PBS containing 100 mM Na_2HPO_4, 18 mM NaH_2PO_4, 2.7 mM KCl and 137 mM NaCl (pH = 7.0) was used. Artificial sweat contained 3 mM NH_4Cl, 22 mM urea, 0.4 mM $CaCl_2$, 50 μM $MgCl_2$, 10 mM KCl, 137 mM NaCl, 25 μM uric acid and 100 μM glucose (pH = 7). All the chemicals were used at least analytical grade without purification process and the Milli-Q water (resistivity more than 18 MΩ/cm) was used in all experiments.

Preparation of elastomeric gold fibers. Firstly, the OA capped ultrathin AuNWs were synthesized by adding $HAuCl_4{\cdot}3H_2O$ (29.3 mg), OA (1 mL) and TIPS (1.4 mL) into n-hexane (30 mL) successively. After keeping solution in dark place at room temperature for more than 12 h, the color of solution was turned from clear red orange into dark red (Figure S1a-b). Afterwards, the AuNWs were centrifuged to remove weakly bonded OA ligand and re-dispersed in THF (2 mL). Then, it was mixed with SEBS (200 mg) and silicon oil (20 mg) by shaking (48 h) and transferred into a syringe. The Au/SEBS elastomeric fibers were obtained by extruding the mixed solution into air, after THF volatilization in room temperature. The obtained fiber with 300% pre-strained was treated by the Au electroless growth solution for 10 min and followed by 25 mM $NaBH_4$ solution for 15 min, respectively. Finally, the elastomeric gold fiber was successfully fabricated after releasing to initial length and the resistance is about 25–50 Ω/cm. With the high conductivity, it can acted as counter electrode directly and can be modified, becoming reference and lactate working electrodes in sensing system.

Preparation of Au/Ag/AgCl reference electrode. A layer of Ag was first electrodeposited onto elastomeric gold fiber surface in 5 mM $AgNO_3$/1 M KNO_3 solution by cyclic voltammetry (CV) scanning from −0.9 to 0.9 V for 14 cycles at 0.1 V/s. The chlorination process was carried out in 10 mM KCl/0.1 M HCl solution using CV scanning from −0.15 to 1.05 V for 4 cycles at 0.05 V/s. Then, a layer of PVB was drop-casted onto the fiber surface to minimize the potential drift [37]. The PVB solution containing 79.1 mg PVB, 50 mg NaCl that dissolved in 1 mL methanol solution.

Preparation of lactate-sensing working electrode. Firstly, a layer of PB was electrodeposited onto elastomeric gold fiber by CV that scan in PB solution (2.5 mM $K_3Fe(CN)_6$ and $FeCl_3$, 0.1 M KCl and HCl) from −0.3 to 0.5 V for 15 cycles at the scan rate of 0.02 V/s. Then, 4 μL of LOx (20 mg/mL) was drop-casted onto it. After drying at room temperature, 8 μL of CS solution (1 wt % CS and 1 wt % acetic acid in water solution) was carefully dropped onto the Au fiber to maintain the activity of LOx (Figure S2). The obtained lactate-sensing working electrodes were obtained after dried in room temperature and it should be stored in 4 °C prior to using.

Wearable lactate textile assembly. As our elastomeric gold fibers are tiny size with hair-like filaments that can be weaved into any kinds of fabrics to be a wearable lactate textile. A fabric from T-shirt was chosen to weave three electrodes into it by needle, keeping as same distance to each fiber and connected to electrochemical station by commercial conductive thread. After each testing, the textile should be dried in room temperature for next testing.

Characterization of sensing fibers. The electrochemical performance of the elastomeric gold fiber was tested by immersing the elastomeric gold fiber into 1 M H_2SO_4 aqueous solution about 1 cm deep and EASA was calculated using CV at 0.1 V/s scan speed. The geometric area (GA) of the fiber surface was calculated via $GA = 2\pi r^* l + \pi r^2$ (r is the diameter of elastomeric fiber, l is the fiber length exposed to solution). The gold fiber was also immersed into 5 mM $KFe(CN)_6^{3-/4-}$ with 0.1 M KCl using CV at 0.1 V/s scan speed under different bending angles 0°–90° from and strain from 0% to 100%. The electrochemical performances of the lactate-sensing system were tested in PBS and artificial sweat by real-time chronoamperometic measurement for 60 s at −0.1 V right after stirring solution for 60 s. Moreover, the selectivity of lactate sensor was tested in PBS solution containing the potential interfering analytes with the final concentration of 0.1 mM glucose, 0.05 mM L-AA, 10 mM NaCl, and 0.05 mM uric acied. The on-body testing was carried out by tied the lactate textile onto volunteer's forearm. On testing, the volunteer (25 year old health male) was asked to running for 15 min, then do intense indoor activity for another 15 min and running for last 15min. The chronoamperometric lactate on-body testing was recorded by electrochemical workstation at −0.1 V for 60s with three conditions, which are 15 min, 30 min and 45 min activities. The smart glove lactate biosensor was used by weaved fiber-based lactate three electrodes into a textile and then restricted it onto the index finger of rubber glove. The smart glove was wore by a volunteer and put the index finger into sample solution which is 0.5 mM, 2 mM and 5 mM lactate in artificial sweat and orange juice solution (pure orange juice diluted 10 times by water). All the electrochemical testing was adopted an electrochemical workstation (Versa STAT, Princeton Applied Research). The structure of fiber was characterized by SEM (FEI Helios Nanolab 600 FIB-SEM) and the structure of OA capped AuNWs was characterized TEM (Philips CM 20). A HPLC experiment was carried out using a 20 mL injection loop and a diode array detector (Agilent 1220 infinity LC). We used a HPLC column MS C18 (XTerra) 150 × 3.0 mm with an isocratic elution in 99% 0.1 M PBS, pH 7.4, 1% methanol flowing at 1.5 mL/min. The chromatographic run was completed in 30 min, including rinsing of the column in 100% methanol and the re-equilibration step. Detection was performed at 210 nm. Firstly, we did an experiments for the standard curve with lactate samples in PBS. Then, the human sweat and orange juice samples were centrifuged and transferred the supernatant to another tube till dried using N_2. The samples were tested after dissolved into PBS as used before.

3. Result and discussion

3.1. Fabrication and characterization of the elastomeric gold fiber

Firstly, elastomeric gold fibers were fabricated by the dry-spinning approach according to the previous reports [29,36]. For fabrication, the OA capped ultrathin AuNWs with a diameter of 2 nm was firstly synthesized by mixing $HAuCl_4$, OA and TIPS into n-hexane [38] under dark condition (Figure S1c). After mixing AuNWs solution with SEBS, silicon oil and THF, the mixture was extruded from syringe into air, leading to spontaneous formation of AuNWs/SEBS fiber. Then, the fiber with 300% pre-strain was immerged into Au electroless growth solution followed by wet nano-welding process ($NaBH_4$ water solution). Since the AuNWs provide nucleation spots for AuNPs generation, it can grow tightly on the fiber surface and it was fused into an Au film with high conductivity. Lastly, after release to initial length, the elastomeric gold fiber could be obtained with wrinkled structures.

The elastomeric gold fibers can be fabricated in large scale with tiny size (Fig. 2a inside) and contained 11 wt% AuNWs. The high gold loading didn't appear to affect elasticity of the fibers as Figure S3 illustrated. As shown in Figure S4a, a huge resistance increasing was observed after strain for gold fiber without pre-strain; while the relative resistance change is only 40% for 300% pre-strained gold fiber under 100% strain level. Although there was some resistance changes (Figure S4b) along with the stretching, the elastomeric gold fiber exhibited superior performance in conductivity, as shown in Fig. 2a. The conductivity at the initial length is about 89 S/cm, which is calculated using following Equation (1):

$$S = \frac{L}{A \times R} \tag{1}$$

where S is the conductivity, L is the length, A is the cross-section area and R is the resistance. The conductivity increased from 89 S/cm to 153

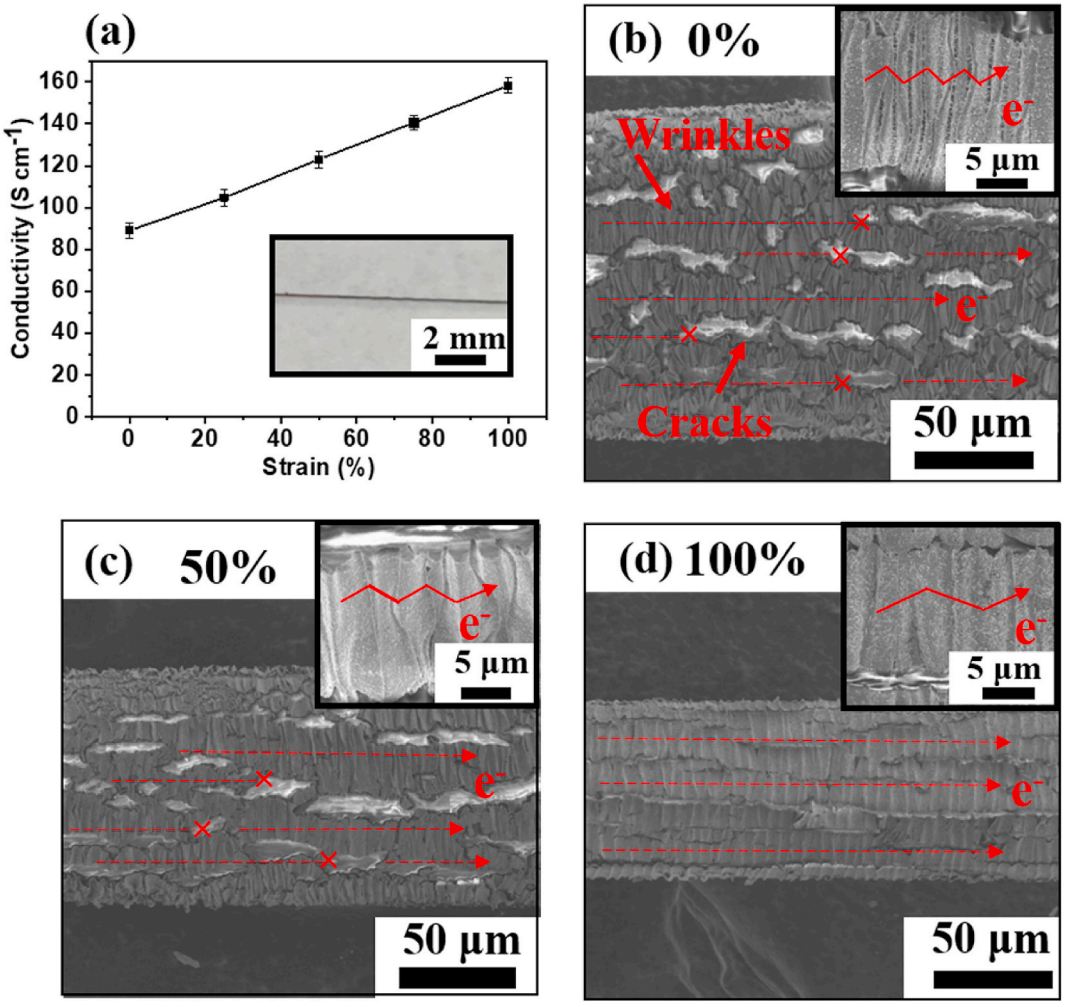

Fig. 2. (a) The conductivity of elastomeric gold fiber at different stretching from 0% to 100%. Inside show that the digital image of the real size of the elastomeric gold fiber. (b) The elastomeric gold fiber at initial length without stretching. Inside show the close packed wrinkled Au film. (c–d) The elastomer gold fiber under 50% and 100% stretching state respectively. Inside show the wrinkled Au film gradually smooth by the increasing stretching. (For interpretation of the references to color in this figure legend, the reader is referred to the Web version of this article.)

S/cm when the fiber was stretched from 0% to 100%. This may be attributed to the sharp shrinkage of the cross-section area of fiber, as the decreased cross-section area is much more significant than the increased resistance [29]. Fig. 2b–d shows the morphological characterization of the fiber under different strains by SEM. One can see that the diameter of the fiber decreased from ~150 μm to ~105 μm–~75 μm when the fiber was stretched from 0% to 50%–100%. The decreased diameter was due to the known positive Poisson's ratio of SEBS, which is 0.49. At unstretched state, cracked gold films were evident (Fig. 2b), simultaneously displaying wrinkled structures as shown in the high-resolution image (**inset of** Fig. 2b) and some cracks were formed by axial expansion during releasing process, which impede electron transport, leading to less conductive pathways though the gold film. Along with the stretching (Fig. 2c and d), the wrinkles were gradually flattened (Fig. 2b–d inside) and the cracks were gradually narrowing via diameter changing (hardly see it at 100% stretching state Fig. 2d), which results in more conductive pathways though the gold film, providing high conductivity at high level of stretching. By using this phenomenon, the elastomeric gold fiber could profit for stretchable electrodes for adaptation to adjust the deformation of normal skin movement.

The wrinkled structure of the Au films might be beneficial for serving as electrochemical biosensing electrodes in that they might offer high electrochemically active surface area (EASA) and facilitate enzyme immobilization [35,39]. We calculated the EASA by immersing the fiber into 1 M H_2SO_4 solution under the CV scanning with a scan rate of 0.1 V/s. As shown in Figure S5, evident gold oxidation and reduction peaks were identified at about 1.3 V and 0.9 V, respectively. The EASA can be then calculated according Equations (2) and (3):

$$EASA = \frac{Q}{c} \tag{2}$$

$$Q = \frac{A}{v} \tag{3}$$

where Q is the required charge for reduction of the Au oxide formed during the positive scan, c is the require charge for the reduction of a monolayer of Au oxide (386 μC/cm^2), A is the reduction peak area and v is the scan rate [40,41]. The estimated EASA is 0.62 cm^2, over 13 times higher than the corresponding geometric area of the fiber surface (0.0471 cm^2).

We further investigated electrochemical performance of elastomeric gold fiber under different bending angles and stretching states using the typical redox probe of $K_3[Fe(CN)_6]/K_4[Fe(CN)_6]$. As shown in Figure S6, there were negligible peak shifts or changes in peak currents under bending angels from 0° to 90°, which demonstrated the bending-insensitive features of our elastomeric gold fiber. As shown in Figure S7a, the characteristic redox peaks of $Fe(CN)_6^{3-/4-}$ were observed under all different levels of strains. Note that the peak-to-peak

separation was insensitive to the change in strain with a negligible variation for the strain range from 0% to 100% (less than 1%). The tiny drifting trend in the peak separation is consistent with the small resistance changes in the absolute resistance as strains were applied (Figure S4b). In contrast, the oxidization and reduction peak currents were highly dependent on the strain level, exhibiting an increasing trend as the strain increase from 118.43 μA to 199.48 μA of oxidation peak and −102.94 μA to −181.88 μA of reduction peak for the stretching level from 0% to 100% (Figure S7b, Table S1). This increasing trend may attribute to the increased exposed surface area of Au film to $Fe(CN)_6^{3-/4-}$ solution, induced by unfolding process of wrinkled structure along with stretching. The more Au participate in a reaction the higher current peaks were observed via CV scanning, which made this elastomeric gold fiber become a promising candidate for stretchable electrochemical electrodes.

3.2. Fabrication and characterization of textile-based lactate biosensors

The as-fabricated elastomeric gold fiber could directly serve as the counter electrode in lactate sensing system, but would need surface modification before their application as reference and working electrodes.

The reference electrode could be prepared by electrodepositing a layer of Ag onto fiber surface followed by chloritization to form AgCl. As shown by SEM images in Figure S8, silver particulate layer could be identified on the surface of wrinkled Au film after Ag electrodeposition process. It also confirmed the presence of Ag and Cl elements on the fiber surface by EDX as shown in Figure S9, in which the brighter areas were

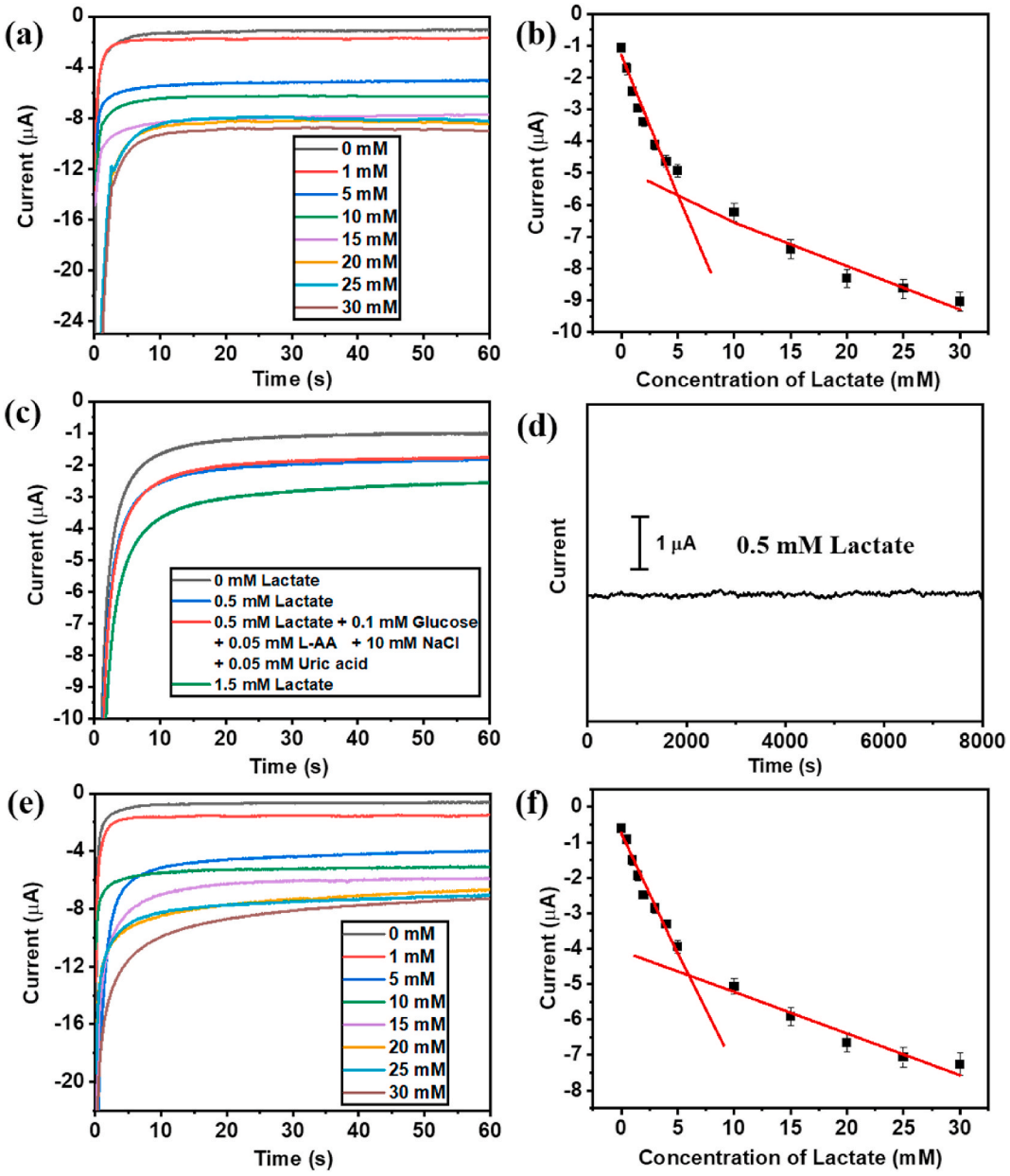

Fig. 3. The performance of wearable lactate textile biosensor in PBS and artificial sweat versus Au/Ag/AgCl reference electrode and elastomeric gold fiber counter electrode using three electrodes chronoamperometry approach at −0.1 V. (a) The sensitivity of lactate textile biosensor to lactate concentration ranged from 0 to 30 mM in PBS. (b) Corresponding calibration plot of lactate biosensor in PBS. (c) The selectivity of lactate textile biosensor in PBS. (d) The operation stability of lactate biosensor at 0.5 mM lactate concentration in PBS. (e) The sensitivity of lactate textile biosensor to lactate concentration ranged from 0 to 30 mM in artificial sweat. (f) Corresponding calibration plot of lactate biosensor in artificial sweat. (For interpretation of the references to color in this figure legend, the reader is referred to the Web version of this article.)

identified to be dominated by Ag elements. An additional layer of PVB coating was applied to the Ag/AgCl modified fiber surface to minimize the potential drift during electrochemical reactions. In contrast, significant potential drift was observed in the absence of PVB coating (Figure S10a). The role of PVB is to maintain a constant concentration of chloride serving as ion-reservoir. Experimentally, we found the PVB membrane was highly effective to maintain stable potential even after adding NaCl (Figure S10b).

The working electrode for the lactate-sensing was prepared through a layer of PB electrodeposition process onto gold fiber surface by CV scan for 15 cycles (Figure S11a). The characteristic redox behavior associated with PB oxidation and reduction was evident in the PBS electrolyte (Figure S11b), which wasn't observed without PB deposition. The PB deposition changed the color of elastomeric gold fiber from golden to dark blue (Figure S12a-b). Finally, the LOx enzyme was drop-casted onto the PB-modified gold fiber followed by a layer of CS to immobilize the enzyme and maintain its bioactivity (Figure S12c). The thus-prepared enzymatic working electrode involves two chemical reactions on the surface of fiber (Fig. 1b). Firstly, the lactate will be oxidized to generate pyruvate and H_2O_2 by LOx in the presence of O_2. Secondly, the PB layer can serve as artificial peroxidase and electron mediator to promote the decomposition of H_2O_2. The PB layer can also promote the electron transport to Au fiber, hence, reducing the potential through redox process.

Once three functional gold fiber electrodes are fabricated, they can be woven into textile fabrics (Fig. 1a). Then, the lactate sensing performance was examined in 0–30 mM lactate PBS buffer (Fig. 3a). At the potential of −0.1 V, the redox current graduated increased following a linear relationship (Fig. 3b). The linear regression gave an estimated sensitivity of 19.13 μA/mM cm^2 (for the concentration range of 0–5 mM, $R^2 = 0.927$, Figure S13) and 2.9 μA/mM cm^2 (for the concentration range of 10–30 mM, $R^2 = 0.91$), respectively and the LOD is 0.137 mM (S/N = 3). The sensing performance was highly specific to lactate. In the control experiment, glucose, L-AA, sodium chloride and uric acid with the similar concentrations in real human sweat were added to the PBS solution. As shown in Fig. 3c, the current increases significantly by addition of lactate, but insensitive to the addition of the interfering chemical species. In addition, the lactate sensor showed good reproducibility for three different individual sensors tested. For the low concentration range, an average sensitivity of 18.59 μA/mM cm^2 and an RSD of 6.3% were achieved (Figure S14a). The as-fabricated textile-based lactate sensor is also highly stable and durable. For the continuous operating of 8000 s in the PBS buffer at room temperature, the current variation was far less than 1 μA (Fig. 3d). With a 6-day storage at 4 °C, the redox current retention still kept about 71% to the initial current (Figure S15).

The electrochemical performance of the lactate textile biosensor was further examined in the formulated artificial sweat that contained NH_4Cl, urea, $CaCl_2$, $MgCl_2$, KCl, NaCl, uric acid and glucose (pH = 7). As shown in Fig. 3e, the redox current increases linearly with the increase of the lactate concentration from 0 mM to 30 mM in the artificial sweat. From Fig. 3f, the linear regression ($R^2 = 0.986$) for the lactate concentration range of 0–5 mM lead to an estimated sensitivity of 14.6 μA/mM cm^2 and 2.5 μA/mM cm^2 (for the concentration range of 0–30 mM, $R^2 = 0.931$). Similar to the sensitivity in PBS, it also showed higher sensitivity in the low lactate concentration range (0–5 mM, Figure S16). The lower sensitivity compared with it in PBS solution was may attribute to the multiple interfering chemical species which could absorbed onto the electrode's surface when working, leading inferior performance compared with PBS solution. Nevertheless, the currents were clear discrimination to different lactate concentration and still maintained relatively high sensitivity in artificial sweat. Moreover, the sensor also showed good repeatability based on the three different sensors tested, achieving an average sensitivity of 14.29 μA/mM cm^2 and an RSD of 5.2% (Figure S14b).

3.3. Sensing performance under strain, on-body sweat analysis and smart glove-based lactate monitoring

For human daily routine activities (the highest strain is about 80% for elbow area), the textile experiences constant mechanical stretching, therefore, it is important to evaluate how our gold fiber-based lactate textile biosensors perform under strains up to 100% (Figure S17). We first examined the sensing performance in the PBS buffer by applying strains from 0% to 100% (Fig. 4a). Encouragingly, the linear relationship was observed in the concentration range of 0–30 mM albeit with biomodal regimes and lower sensitivities under stretched states. This may be attributed to the strain-insensitive properties of elastomeric gold fiber which is able to maintain conductivities under this level of strains. Note that our elastomeric sensors displayed linear behaviors for all these different strain levels, especially keeping the high sensitivity in the low lactate concentration range (Figure S18a). The sensitivities at these stretched states from 25% to 100% showed a small variation of 7.5% for low concentration range (0–5 mM) and 5.9% for high concentration range (10–30 mM), which had negligible impact on the lactate sensing. This small degradation of sensitivities might be caused due to the change in electroactive surface areas of gold fiber under stretched states.

The electrochemical performance of wearable lactate textile biosensor was also investigated under strains up to 100% in the artificial sweat. As shown in Fig. 4b, the similar strain-tolerant sensitivity was observed. In the lactate concentration regime of 0–30 mM, the elastomeric gold fibers showed the good linear relationships for all the strain levels, which were not too much affected by the interfering substances present in the artificial sweat. Although the sensitivity (0–5 mM, Figure S18b and 10–30 mM, Fig. 4b) at stretched states (25%–100%) were lower than that for unstretched state, it still could discriminate different lactate concentration up to 30 mM. Furthermore, the ratio of current retention of wearable lactate textile biosensor after different stretching cycles (30%) were also investigated at 0.5 mM lactate concentration in the artificial sweat, as shown in Figure S19. After 100 stretching cycles, the current retention was about 88%. In addition, we compared the sensing performance of our lactate biosensor with other reported lactate biosensors in the literatures as shown in Table S2. It shows that our gold fiber-based lactate biosensors offer the excellent sensitivity and the high stretchability simultaneously.

As a proof-of-concept application, we further applied our lactate textile sensors attaching onto the forearm of volunteer for on-body sweat analysis to investigate how human physical exercises changed the lactate concentration in sweat (Fig. 4c). Our sensor identified redox current at 15 min after the physical exercise (Figure S20). The current increased at 30 min after the physical exercise. However, the lactate concentration decreased at 45 min after the exercises, which was due to the dilution factor expected after the physical exercise (the increased sweat production could decrease the lactate concentration in the condition of extremely strong exercise intensities). The lactate concentration were calculated based on the calibration curve in Fig. 3f and showed in Fig. 4d. To confirm lactate concentration in sweats, we measured lactate concentrations with HPLC [42]. It showed an obvious discrepancy between our textile fiber sensors and HPLC. While sweat collection has been known to be a complex issue in wearable diagnostics, we believe it might be due to concentration variation from skin surface to sensor given a thickness of textile cloth of ~1 mm (Figure S21 **and associated discussions)**. Nevertheless, the trend in the change of lactate concentration observed in our experiment were in agreement with the literature [43]. It is well-known that sweat collection/sampling is a challenging issue for accurate sweat analysis due to the complication in individual sweat rates, sweat-collecting substrate (tissue paper, textile, skin contactability, concentration gradient, etc.). In this context, the textile-based wearable lactate biosensor may offer the high wearing comfortability, which is highly desired for noninvasive lactate monitoring from human sweat as a semi-quantitative assessment tool.

We further extended our gold fiber-based textile design to potential

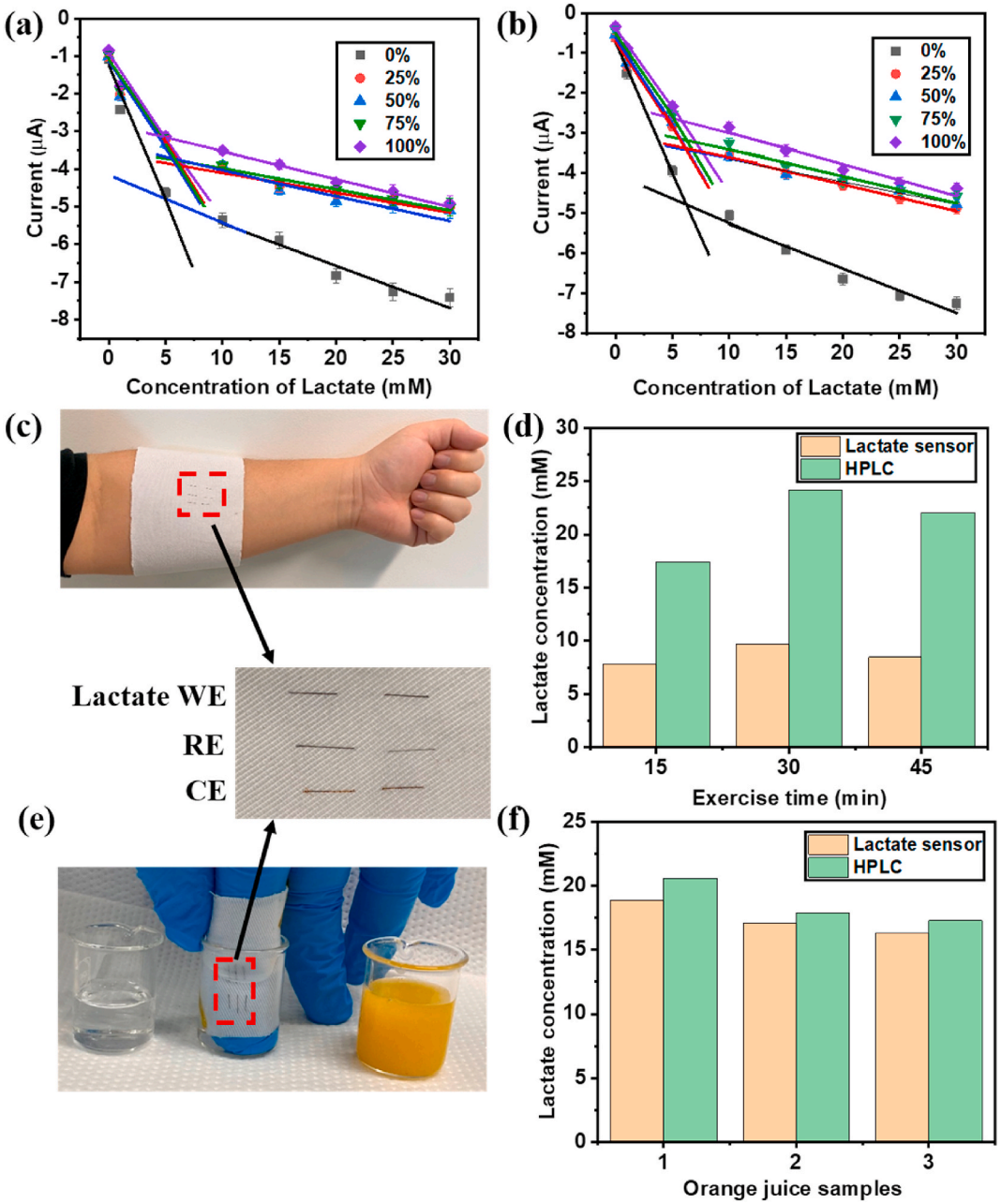

Fig. 4. (a) The liner relationship of fiber-based lactate textile biosensor at 0%–100% stretching states in different lactate concentration ranged from 0 mM to 30 mM in PBS and artificial sweat (b). (c) The digital image of wearable lactate textile biosensor attached onto volunteer's forearm, contacting three fiber electrodes system for lactate testing. (d) The on-body sweat lactate testing at 15 min, 30 min and 45 min physical exercise conditions compared with HPLC results. (e) The digital image of glove-based lactate biosensor attached onto index finger of rubber glove and different testing samples (Left and middle: 0.5 mM and 5 mM lactate in artificial sweat; Right: orange juice). (f) The lactate concentration tested by three pure orange juice samples compared with HPLC results. (For interpretation of the references to color in this figure legend, the reader is referred to the Web version of this article.)

robotic fingertip biosensor for sweat analysis and detecting "food content" [44]. As shown in Fig. 4e, a volunteer wore the textile sensor onto the index finger and detected lactate concentration in the artificial sweat and orange juice solution. From Figure S22, the lactate concentrations of sample 1 to sample 3 (S1, S2 and S3) were clear shown after testing, corresponding to a lactate concentration based on the calibration curve in Figure S16, which are very close to the concentration that calibrated. Then, a commercial pure orange juice was also tested after diluting 10 times. As shown in Fig. 4f and Figure S23, the average lactate concentration from 3 samples in this juice was about 17.43 mM based on the calibration curve in Fig. 3f. It was consistent with the average lactate concentration estimated from HPLC measurement (18.57 mM). Thus, the robotic fingertip lactate biosensor could potentially be used to monitor lactate concentration from any type of samples including juice, leading potential application in soft robotic area in near future.

4. Conclusion

To sum up, we have demonstrated a wearable fiber-based smart textile electrochemical lactate biosensing device, which can be acted as a wearable non-invasive platform for wearing. Using lactate as a typical biomarker in human sweat, the enzyme-based amperometric biosensor have shown excellent detection performances toward lactate in sensitivity of 19.13 μA/mM cm^2 in PBS and 14.6 μA/mM cm^2 in artificial

sweat, selectivity, linear range (0 mM–30 mM), LOD (0.137 mM) and stretchability up to 100%. This proof-of-concept demonstration indicates the potential of our gold fiber-based textile platform for applications for non-invasive, point-of-care and real-time lactate monitoring and robotic sensing.

Credit author statement

Ren Wang: Experimental data collection and analysis, Writing-Original draft preparation. Qingfeng Zhai: Experimental data collection and analysis. Tiance An: Experimental data collection and analysis. Shu Gong: Experimental data collection and analysis. Wenlong Cheng: Supervision, Conceptualization, Data Analysis, Writing- Reviewing and Editing.

Declaration of competing interest

The authors declare that they have no known competing financial interests or personal relationships that could have appeared to influence the work reported in this paper.

Acknowledgements

This research was financially supported under Australian Research Council's discovery Projects funding scheme (DP180101715 and DP170102208). This work was performed in part at the Melbourne Centre for Nanofabrication (MCN) in the Victorian Node of the Australian National Fabrication Facility (ANFF). We also thanks Mr Waqar Ahmad and A/Prof Akshat Tanksale for assisting HPLC characterizations.

Appendix A. Supplementary data

Supplementary data to this article can be found online at https://doi.org/10.1016/j.talanta.2020.121484.

References

[1] J. Kim, A.S. Campbell, B.E. de Avila, J. Wang, Wearable biosensors for healthcare monitoring, Nat. Biotechnol. 37 (4) (2019) 389–406.
[2] M. Bariya, H.Y.Y. Nyein, A. Javey, Wearable sweat sensors, Nat. Electron. 1 (3) (2018) 160–171.
[3] Y. Yang, W. Gao, Wearable and flexible electronics for continuous molecular monitoring, Chem. Soc. Rev. 48 (6) (2019) 1465–1491.
[4] T. Someya, M. Amagai, Toward a new generation of smart skins, Nat. Biotechnol. 37 (4) (2019) 382–388.
[5] S.T. Han, H. Peng, Q. Sun, S. Venkatesh, K.S. Chung, S.C. Lau, Y. Zhou, V.A.L. Roy, An overview of the development of flexible sensors, Adv. Mater. 29 (33) (2017).
[6] H. Lee, C. Song, Y.S. Hong, M.S. Kim, H.R. Cho, T. Kang, K. Shin, S.H. Choi, T. Hyeon, D.H. Kim, Wearable/disposable sweat-based glucose monitoring device with multistage transdermal drug delivery module, Sci. Adv. 3 (3) (2017), e1601314.
[7] X. He, T. Xu, Z. Gu, W. Gao, L.P. Xu, T. Pan, X. Zhang, Flexible and superwettable bands as a platform toward sweat sampling and sensing, Anal. Chem. 91 (7) (2019) 4296–4300.
[8] C. Liu, T. Xu, D. Wang, X. Zhang, The role of sampling in wearable sweat sensors, Talanta 212 (2020) 120801.
[9] F. Alam, S. RoyChoudhury, A.H. Jalal, Y. Umasankar, S. Forouzanfar, N. Akter, S. Bhansali, N. Pala, Lactate biosensing: the emerging point-of-care and personal health monitoring, Biosens. Bioelectron. 117 (2018) 818–829.
[10] K. Rathee, V. Dhull, R. Dhull, S. Singh, Biosensors based on electrochemical lactate detection: a comprehensive review, Biochem. Biophys. Rep. 5 (2016) 35–54.
[11] W. Jia, A.J. Bandodkar, G. Valdes-Ramirez, J.R. Windmiller, Z. Yang, J. Ramirez, G. Chan, J. Wang, Electrochemical tattoo biosensors for real-time noninvasive lactate monitoring in human perspiration, Anal. Chem. 85 (14) (2013) 6553–6560.
[12] J. Kim, G. Valdes-Ramirez, A.J. Bandodkar, W. Jia, A.G. Martinez, J. Ramirez, P. Mercier, J. Wang, Non-invasive mouthguard biosensor for continuous salivary monitoring of metabolites, Analyst 139 (7) (2014) 1632–1636.
[13] S. Imani, A.J. Bandodkar, A.M. Mohan, R. Kumar, S. Yu, J. Wang, P.P. Mercier, A wearable chemical-electrophysiological hybrid biosensing system for real-time health and fitness monitoring, Nat. Commun. 7 (2016) 11650.
[14] S. Anastasova, B. Crewther, P. Bembnowicz, V. Curto, H.M. Ip, B. Rosa, G.Z. Yang, A wearable multisensing patch for continuous sweat monitoring, Biosens. Bioelectron. 93 (2017) 139–145.
[15] W. He, C. Wang, H. Wang, M. Jian, W. Lu, X. Liang, X. Zhang, F. Yang, Y. Zhang, Integrated textile sensor patch for real-time and multiplex sweat analysis, Sci. Adv. 5 (11) (2019) eaax0649.
[16] W. Gao, S. Emaminejad, H.Y.Y. Nyein, S. Challa, K. Chen, A. Peck, H.M. Fahad, H. Ota, H. Shiraki, D. Kiriya, D.H. Lien, G.A. Brooks, R.W. Davis, A. Javey, Fully integrated wearable sensor arrays for multiplexed in situ perspiration analysis, Nature 529 (7587) (2016) 509–514.
[17] J. Kim, I. Jeerapan, J.R. Sempionatto, A. Barfidokht, R.K. Mishra, A.S. Campbell, L. J. Hubble, J. Wang, Wearable bioelectronics: enzyme-based body-worn electronic devices, Acc. Chem. Res. 51 (11) (2018) 2820–2828.
[18] W. Gao, H. Ota, D. Kiriya, K. Takei, A. Javey, Flexible electronics toward wearable sensing, Acc. Chem. Res. 52 (3) (2019) 523–533.
[19] W. Weng, P. Chen, S. He, X. Sun, H. Peng, Smart electronic textiles, Angew. Chem., Int. Ed. Engl. 55 (21) (2016) 6140–6169.
[20] W. Zeng, L. Shu, Q. Li, S. Chen, F. Wang, X.M. Tao, Fiber-based wearable electronics: a review of materials, fabrication, devices, and applications, Adv. Mater. 26 (31) (2014) 5310–5336.
[21] J. Lee, B. Llerena Zambrano, J. Woo, K. Yoon, T. Lee, Recent advances in 1D stretchable electrodes and devices for textile and wearable electronics: materials, fabrications, and applications, Adv. Mater. (2019), e1902532.
[22] X. Liu, P.B. Lillehoj, Embroidered electrochemical sensors for biomolecular detection, Lab Chip 16 (11) (2016) 2093–2098.
[23] M. Tessarolo, I. Gualandi, B. Fraboni, Recent progress in wearable fully textile chemical sensors, Adv. Mater. Technol. 3 (10) (2018).
[24] L. Wang, X. Fu, J. He, X. Shi, T. Chen, P. Chen, B. Wang, H. Peng, Application challenges in fiber and textile electronics, Adv. Mater. 32 (5) (2020), e1901971.
[25] L. Wang, L. Wang, Y. Zhang, J. Pan, S. Li, X. Sun, B. Zhang, H. Peng, Weaving sensing fibers into electrochemical fabric for real-time health monitoring, Adv. Funct. Mater. 28 (42) (2018).
[26] J.R. Sempionatto, T. Nakagawa, A. Pavinatto, S.T. Mensah, S. Imani, P. Mercier, J. Wang, Eyeglasses based wireless electrolyte and metabolite sensor platform, Lab Chip 17 (10) (2017) 1834–1842.
[27] S. Gong, Y. Zhao, L.W. Yap, Q. Shi, Y. Wang, J.A.P.B. Bay, D.T.H. Lai, H. Uddin, W. Cheng, Fabrication of highly transparent and flexible NanoMesh electrode via self-assembly of ultrathin gold nanowires, Adv. Electron. Mater. 2 (7) (2016).
[28] Y. Wang, S. Gong, S.J. Wang, X. Yang, Y. Ling, L.W. Yap, D. Dong, G.P. Simon, W. Cheng, Standing enokitake-like nanowire films for highly stretchable elastronics, ACS Nano 12 (10) (2018) 9742–9749.
[29] Y.M. Zhao, D.S. Dong, S. Gong, L. Brassart, Y. Wang, T. An, W.L. Cheng, A moss-inspired electroless gold-coating strategy toward stretchable fiber conductors by dry spinning, Adv. Electron. Mater. 5 (1) (2019).
[30] S. Gong, L.W. Yap, B. Zhu, Q. Zhai, Y. Liu, Q. Lyu, K. Wang, M. Yang, Y. Ling, D.T. H. Lai, F. Marzbanrad, W. Cheng, Local crack-programmed gold nanowire electronic skin tattoos for in-plane multisensor integration, Adv. Mater. 31 (41) (2019), e1903789.
[31] B. Zhu, S. Gong, W. Cheng, Softening gold for elastronics, Chem. Soc. Rev. 48 (6) (2019) 1668–1711.
[32] Q. Zhai, W. Cheng, Soft and stretchable electrochemical biosensors, Mater. Today Nano 7 (2019).
[33] Q. Zhai, S. Gong, Y. Wang, Q. Lyu, Y. Liu, Y. Ling, J. Wang, G.P. Simon, W. Cheng, Enokitake mushroom-like standing gold nanowires toward wearable noninvasive bimodal glucose and strain sensing, ACS Appl. Mater. Interfaces 11 (10) (2019) 9724–9729.
[34] Q. Zhai, L.W. Yap, R. Wang, S. Gong, Z. Guo, Y. Liu, Q. Lyu, J. Wang, G.P. Simon, W. Cheng, Vertically aligned gold nanowires as stretchable and wearable epidermal ion-selective electrode for noninvasive multiplexed sweat analysis, Anal. Chem. 92 (6) (2020) 4647–4655.
[35] Y. Zhao, Q. Zhai, D. Dong, T. An, S. Gong, Q. Shi, W. Cheng, Highly stretchable and strain-insensitive fiber-based wearable electrochemical biosensor to monitor glucose in the sweat, Anal. Chem. 91 (10) (2019) 6569–6576.
[36] R. Wang, Q. Zhai, Y. Zhao, T. An, S. Gong, Z. Guo, Q. Shi, Z. Yong, W. Cheng, Stretchable gold fiber-based wearable electrochemical sensor toward pH monitoring, J. Mater. Chem. B 8 (16) (2020) 3655–3660.
[37] T. Guinovart, G.A. Crespo, F.X. Rius, F.J. Andrade, A reference electrode based on polyvinyl butyral (PVB) polymer for decentralized chemical measurements, Anal. Chim. Acta 821 (2014) 72–80.
[38] S. Gong, W. Schwalb, Y. Wang, Y. Chen, Y. Tang, J. Si, B. Shirinzadeh, W. Cheng, A wearable and highly sensitive pressure sensor with ultrathin gold nanowires, Nat. Commun. 5 (2014) 3132.
[39] Q. Zhai, Y. Wang, S. Gong, Y. Ling, L.W. Yap, Y. Liu, J. Wang, G.P. Simon, W. Cheng, Vertical gold nanowires stretchable electrochemical electrodes, Anal. Chem. 90 (22) (2018) 13498–13505.
[40] S. Trasatti, O.A. Petrii, Real surface area measurements in electrochemistry, Pure Appl. Chem. 63 (5) (1991) 711–734.
[41] F. Jia, C. Yu, Z. Ai, L. Zhang, Fabrication of nanoporous gold film electrodes with ultrahigh surface area and electrochemical activity, Chem. Mater. 19 (15) (2007) 3648–3653.
[42] S. Biagi, S. Ghimenti, M. Onor, E. Bramanti, Simultaneous determination of lactate and pyruvate in human sweat using reversed-phase high-performance liquid chromatography: a noninvasive approach, Biomed. Chromatogr. 26 (11) (2012) 1408–1415.
[43] M.J. Buono, N.V. Lee, P.W. Miller, The relationship between exercise intensity and the sweat lactate excretion rate, J. Physiol. Sci. 60 (2) (2010) 103–107.
[44] L.J. Hubble, J. Wang, Sensing at your fingertips: glove-based wearable chemical sensors, Electroanalysis 31 (3) (2018) 1–10.